



<https://theses.gla.ac.uk/>

Theses Digitisation:

<https://www.gla.ac.uk/myglasgow/research/enlighten/theses/digitisation/>

This is a digitised version of the original print thesis.

Copyright and moral rights for this work are retained by the author

A copy can be downloaded for personal non-commercial research or study,
without prior permission or charge

This work cannot be reproduced or quoted extensively from without first
obtaining permission in writing from the author

The content must not be changed in any way or sold commercially in any
format or medium without the formal permission of the author

When referring to this work, full bibliographic details including the author,
title, awarding institution and date of the thesis must be given

Enlighten: Theses

<https://theses.gla.ac.uk/>
research-enlighten@glasgow.ac.uk

SOME ASPECTS OF STEADY AND ACCELERATED MOTION
OF ROTATING VISCOUS FLUIDS.

SUMMARY:

An apparatus and its associated instrumentation, designed and built to study problems related to steady-state and accelerated motion of rotating fluids are described.

Experiments were conducted within the limitations of the existing equipment to determine the effectiveness and reliability of the combined unit. Both sets of experiments were run under steady-state conditions.

Through a theoretical treatment by Stokes and Brodmann in which the couple exerted on one cylinder is shown to be a function of the speed of the other, the fluid viscosity, and the cylinder radii, it was found that an additional calibration was required before quantitative results could be obtained. The experiments, however, indicated excellent repeatability - suggesting little random error and the probability of reliable data once the calibration was completed.

The equipment was used in the second group of experiments to detect the onset of fluid instability - characterized by an increase in the frictional couple exerted on the fluid boundaries. It was possible to detect unstable conditions, however, lack of sensitivity in the/

ProQuest Number: 10647695

All rights reserved

INFORMATION TO ALL USERS

The quality of this reproduction is dependent upon the quality of the copy submitted.

In the unlikely event that the author did not send a complete manuscript and there are missing pages, these will be noted. Also, if material had to be removed, a note will indicate the deletion.



ProQuest 10647695

Published by ProQuest LLC (2017). Copyright of the Dissertation is held by the Author.

All rights reserved.

This work is protected against unauthorized copying under Title 17, United States Code
Microform Edition © ProQuest LLC.

ProQuest LLC.
789 East Eisenhower Parkway
P.O. Box 1346
Ann Arbor, MI 48106 – 1346

the existing instrumentation prevented the recording of absolute values.

With suitably-prepared solutions, the onset of instability, expressed as a ratio, was determined visually to within $\pm 2\%$ of the estimated value.

A theoretical analysis by Professor T. H. Havelock forms the basis for proposed experiments in accelerated motion. In the paper, Havelock considers the motion of a hollow cylinder containing a viscous fluid being accelerated from rest under the action of a constant torque. A non-dimensional representation of the relevant parameters is suggested in the present paper as a means of comparing theoretical and experimentally determined results. In order to simplify computation of the theoretical solution, a programme was written for the "DEUCE" computer, and using a typical, but hypothetical set of values, a set of curves was produced.

A discussion of the theoretical solution and of probable experimental results is given, followed by a suggested course of future programme.

↘

SOME ASPECTS OF STEADY AND ACCELERATED
MOTION OF ROTATING VISCOUS FLUIDS

↑

W.R. TUCKER

This thesis was submitted on application for the degree of M.Sc. (Eng.). The work was carried out in the Department of Aeronautics and Fluid Mechanics in the Engineering Faculty of Glasgow University.

The author would like to express his thanks to Professor T.R.F. Nonweiler, Dr. A.S. Thom, Mr. P.H. Tanner, and Dr. D. Morrison for their assistance during the course of the work. He is also grateful to Mr. A.W. Connell, Mr. W. Page, and the staff of the Fluids Division of the National Engineering Laboratory for their contributions to the apparatus.

INDEX

1.	INTRODUCTION.....	1
2.	DESCRIPTION OF THE APPARATUS AND INSTRUMENTATION.....	2
2.1	THE APPARATUS.....	2
2.2	INSTRUMENTATION.....	5
2.21	Torque.....	5
2.22	Cylinder Speed and Acceleration.....	7
2.23	Temperature.....	8
3.	STEADY-STATE MOTION.....	9
3.1	OBSERVATIONS AND RESULTS.....	16
3.11	Laminar Flow.....	16
3.12	Stability Experiments.....	19
3.2	SUMMARY OF STEADY-STATE EXPERIMENTS.....	23
4.	ACCELERATED FLOW.....	24
4.1	PROPOSED EXPERIMENTS.....	24
4.2	GENERAL DISCUSSION.....	28
4.3	FUTURE PROGRAMME.....	32

FIGURES

APPENDICES

REFERENCES

1. INTRODUCTION

During the last century a considerable amount of time and effort has been devoted, by both physicists and engineers, to the problems related to the study of hydrodynamics. Particular attention has been given to a number of subjects within this category - one of these being concerned with the characteristics of flows associated with cylindrical fluid motion.

Basically, the majority of the problems solved have been similar, in that, the theoretical solution has involved the interaction of the fluid, represented by the standard hydrodynamic equations written in cylindrical-polar co-ordinates, with the fluid boundaries expressed by a given set of conditions. The theoretical analyses, in most cases, have been verified by extensive experimental work, resulting in readily predictable phenomena for a wide variety of imposed boundary controls. This is certainly true of most of the flows concerned with steady-state cylindrical motion.

However the study of accelerated motion in this category has received relatively little attention, and of the theoretical analyses which have been proposed,

few have been verified experimentally.

It was therefore decided to construct an apparatus not only capable of reproducing the known results of a variety of problems under steady-state conditions, but also suitable for investigating some of the problems associated with accelerated fluid motion.

2. DESCRIPTION OF THE APPARATUS AND INSTRUMENTATION

2.1 THE APPARATUS

The apparatus selected to perform the set of experiments consisted of a drive assembly coupled to two cylinders mounted, one inside the other, on a pair of parallel axes. The central unit of the drive assembly was a Brookhirst Igronic induction clutch. Power was supplied to the input side of the clutch by a 2 HP., 2850 RPM induction motor, while the output led through a spiral-bevel gear configuration to a pair of shafts, which in turn were belt-connected to the two cylinders.

The gear arrangement permitted independent cylinder rotation, in the same, or opposite directions. The two cylinders could be rotated at different relative speeds by altering the belt-pulley ratios.

The cylinder assembly was built around the 2 ft. long 'Pyrex' glass cylinder which formed the outer cylinder. This cylinder had ground surfaces at both ends, which were parallel to the cylinder axis - thus ensuring concentricity with the remainder of the apparatus once assembled. (Selection of a glass cylinder enabled the fluid motion to be observed; however, where this was not of interest, a metallic cylinder could be substituted.) Compressed 'O'-Rings formed the connection between the metallic and glass components of the outer cylinder assembly.

Magnesium alloy was chosen for the inner cylinder and the metallic portion of the outer assembly. The main reason for using this material was to gain the benefits from its relatively low density. The light weight of the material enabled the inertia of the system to be minimized, thus reducing the torques required for any given acceleration.

Only the smallest clutch in the range manufactured would respond to the type of dual-purpose control desired for the experiments, and the low torques associated with the lower inertias enabled the clutch to be used within its rated torque and heat dissipation requirements.

As all of the experiments were run with water, water-"Pluracol", or water-glycerin solutions, the non-corrosive properties of the magnesium alloy were also used to advantage.

The magnesium inner cylinder was designed to run in two ball bearings; one rigid, the other self-aligning, and both bearings were housed in the outer-cylinder assembly. Sufficient clearance was left in the bearing housings to allow the inner cylinder to be run eccentrically.

Adjacent to the lower self-aligning bearing were the lip-seal, which retained the working fluid, and a gland which enabled the bearing and seal to be rigidly fixed once the cylinder alignment had been established.

The upper limit of rotational speed of the two cylinders was set at 4000 RPM - the allowable maximum for the bearings. Calculation of the inner and outer assembly critical speeds by the method shown in Appendix II, showed lower critical speeds of approximately 5,700 and 11,000 RPM respectively, thus enabling use of the complete speed range.

A sliding fit between the inner cylinder and its upper bearing not only provided for any temperature

effects on the inner cylinder, but, by means of a spring washer-and-screw arrangement, enabled loading of the four bearings on the apparatus. The apparatus was fixed in position through the two outer cylinder bearings. The mountings, in which the assembly sat, were slotted to enable a change of working fluid without affecting the relative cylinder alignment. Two holes in the metallic portion of the outer cylinder, directly above the glass cylinder, allowed for the filling and emptying of the annulus.

2.2 INSTRUMENTATION

The instrumentation which was selected for the apparatus was primarily chosen for its application to accelerated-flow experiments. By the nature of these experiments, four quantities; torque, cylinder speed, acceleration and temperature were to be detected and recorded. The instruments selected for each purpose will be described individually.

2.21 Torque:

Saunders-Roe Torsion-Sensitive Foil Gauges were used to determine the torques supplied to the cylinders. A section between the drive input and the working area,

on both assemblies, was turned to a diameter corresponding to an even number of paired gauge elements.

The gauges were assembled and wired as four equal active arms of a Wheatstone Bridge. The connections to the various arms were such as to provide strains of opposite sign in adjacent bridge arms, thus obtaining four times the output signal associated with a single active gauge.

The bridge was energized by an A-C carrier-amplifier system which provided a 4 volt RMS signal of 3 KC/sec. frequency. The signal was applied to the bridge through a set of miniature slip-ring and brush units which were mounted at the end of each cylinder.

The basic principle of the system was as follows. An out of balance in the Bridge circuit modulated the carrier-frequency. The signal was amplified, and then demodulated - the resulting output being proportional to the bridge unbalance. This output was to be used for two purposes.

Figure 1 shows a static-calibration of torque on the outer cylinder against the corresponding gauge output, as represented by a deflection on an ultra-violet galvanometer recorder. This enabled the values of static

as well as dynamic torque on the cylinder to be determined.

For the first experiments planned in accelerated fluid motion which are discussed later in this thesis, a constant cylinder driving torque is required. The circuit designed to produce this result is at present being developed in the Electrical Engineering Department at the University, and basically uses an amplified error signal from the strain-gauge bridge to feed a transistorized circuit which, in turn, monitors the current into the induction clutch.

2.22 Cylinder Speed and Acceleration:

The problem of speed control and the recording of both cylinder speed and acceleration was similar to that encountered in the case of torque. A circuit, shown schematically in Figure 2, was designed and developed by A. Connell of the Electrical Engineering Department, and used an error signal originating from a phonic wheel, mounted on the rotating cylinder, as a means of controlling the input current to the clutch.

For experiments involving constant speed, pulses from the phonic wheel were fed directly into an electronic counter - from which a continuous reading could be

obtained. However, for the experiments involving accelerated motion, both speed and acceleration values will be required with respect to time, and in these cases the galvanometer recorder could be used. The diode-pump integrator produces an output voltage varying linearly with frequency (and hence speed), and therefore a straight forward calibration of deflection versus frequency would determine the speed. A physical or electrical differentiation of the speed versus time recorder trace in the acceleration experiments would yield the acceleration at any speed - variable sensitivity being obtainable on the time base by altering the paper speed of the recorder.

2.23 Temperature:

Ideally, recording of the fluid temperature should have occurred simultaneously with the measurements of torque, speed and acceleration. However, the complications involved in installing the temperature sensing device were considerable, and therefore a method of measurement was adopted where the fluid temperature before and after an experiment was taken.

The sensing device chosen was a Nichrome-Constantan thermocouple, in which the first three feet of wire from

the junction was enclosed in PVC tubing, so as to allow the junction to be lowered to the base of the cylinders. A potentiometer-galvanometer circuit was used in conjunction with the thermocouple; the actual temperature values being obtained from the National Engineering Laboratory's calibration of the wire, shown in Figure 3. This enabled the temperature to be recorded to an accuracy of $\pm 0.1^{\circ}\text{C}$.

Figure 4 shows the cylinder arrangement and the drive unit, while Figure 5 represents the general layout of the apparatus and associated instrumentation.

5. STEADY-STATE MOTION

5. STEADY-STATE MOTION

Of the numerous types of experiment possible in the study of steady rotation of a viscous liquid, two will be considered - each of which was selected for a particular reason.

Perhaps the best known, and undoubtedly one of the most practical of the experiments in this category, concerns the use of concentric cylinders as a means of determining fluid viscosity. A theoretical treatment by Stokes and by Brodmann has shown that when one of the cylinders is rotated at a constant angular velocity, the

couple exerted on the other, held stationary, can be expressed in the form:

$$G = \frac{4\pi\mu R_1^2 R_2^2 \Omega_1 h}{R_2^2 - R_1^2} \quad (1)$$

where:

G is the couple on the outer cylinder.

μ is the dynamic viscosity of the fluid.

Ω_1 is the angular velocity of the rotating cylinder.

R_1 is the inner cylinder radius.

R_2 is the outer cylinder radius.

h is the length of the outer cylinder.

Through this expression, therefore, it was possible to determine the effectiveness of the apparatus and instrumentation as suitable results were dependent on a combination of the three variables - speed, torque and temperature.

The above expression is valid when the flow between the cylinders is laminar, but fails to be valid once turbulent conditions exist. Donnelly and Simon⁽¹⁾ have derived an empirical relationship by fitting a mathematical curve to known experimental results. The expression:

$$G = a\Omega^{-1} + b\Omega^{1.36}$$

gives values of torque on a stationary outer cylinder as a function of the angular velocity of the inner cylinder for flows extending from the onset of the laminar breakdown well into the turbulent flow range.

The second group of experiments were conducted in an attempt to use the instrumentation which was available on the apparatus, to detect the change in fluid friction associated with the transition of flow which occurs between rotating co-axial cylinders. The subject of instability of this type of flow will be referred to later in this paper, and therefore before describing the actual experiments, an outline of the underlying theory on this topic will be given.

The stability of steady circular flow of a fluid between rotating cylinders, or Couette flow, has received a considerable amount of attention - both in the theoretical and experimental aspect of the study. Basically, the entire problem of stability of this type of flow is centred around the quantity angular momentum, as potential instability has been found to stem directly from an unfavorable gradient of this quantity.

A criterion, proposed by Rayleigh, forms the basis for the study and expression of unstable Couette

flow, and, although originally argued for the case of an incompressible inviscid fluid, the criterion, altered slightly to include the effect of viscosity, provides a centre around which the entire study revolves. (2)

Rayleigh's criterion states: "in the absence of viscosity, the necessary and sufficient condition for a distribution of angular velocity to be stable is for $\frac{\partial}{\partial r} (r\Omega)^2 > 0$ everywhere in the interval - Ω representing the angular velocity at any radius 'r'."

As well as treating the problem through a rigorous mathematical analysis, Chandrasekhar has shown effectively the application of Rayleigh's criterion to viscous steady flow between cylinders when the distribution of angular velocity is restricted to the form $\Omega(r) = A + B/r^2$. The expression produced is in the form of a non-dimensional number, which Chandrasekhar calls, the "Taylor Number", written:

$$T = \frac{4\Omega_1^2 R_1^4}{\nu^2} \frac{(1-u)(1-u/n^2)}{(1-n^2)^2}$$

where:

T represents the Taylor Number.

Ω_1 represents the angular velocity of the inner cylinder.

R_1 represents the inner cylinder radius.

ν represents the kinematic viscosity.

u represents the ratio of the cylinder angular velocities = $\left(\frac{\Omega_2}{\Omega_1}\right)$.

n represents $\left(\frac{R_1}{R_2}\right)$ the ratio of the cylinder radii.

It has been shown, both theoretically and experimentally, that, when conditions satisfy Lord Rayleigh's criterion in a viscous fluid, then the flow is definitely stable. Therefore, when: $\frac{\Omega_2}{\Omega_1} > \left(\frac{R_1}{R_2}\right)^2$, the

flow is always stable.

However, for $\frac{\Omega_2}{\Omega_1} < \left(\frac{R_1}{R_2}\right)^2$, the flow can either be stable or unstable, depending on the value of the Taylor Number, or equivalent expression.

The analytical study of stability in Couette flow, therefore, is concentrated on finding the value of this number, or its equivalent, which corresponds to the onset of instability. (2), (3) The solution is, in all cases, the result of solving the relevant perturbation equations (i.e. the basic hydrodynamic equations written in terms of the perturbed state.)

A set of equations evolve, which for given values of 'u' and 'n' can be reduced to two variables - Taylor Number or its equivalent, and an expression which is related to the wavelength of the disturbance in the axial direction.

The solution of these equations is one of trial and error, and involves finding the value of a wavelength which will yield a minimum value of $\left\{\frac{\Omega_1}{V}\right\}$ - this value then corresponding to the critical $\left\{\frac{\Omega_1}{V}\right\}$ ratio above which instability will occur. The instability is accompanied by the formation of a system of vortices, known as Taylor vortices, whose distribution and dimensions are directly related to the wavelength corresponding to critical conditions.

In previous experimental work, two methods have been used successfully to determine the onset of instability - the method adopted usually depending upon the limitations of the experimental instrumentation. The earlier experimenters observed the breakdown visibly. However, more recently, critical conditions have been detected by making use of the increase in fluid friction which is known to occur at the onset of unstable flow.

The method chosen to observe and record this phenomenon in the present group of experiments differed slightly from the previous techniques used. Since the apparatus was equipped with a constant-speed control, and a suitable method of determining torque, but had no means of controlling the fluid temperature, the following method was adopted. For given ratios of cylinder radii and angular velocity, a value corresponding to the critical $\left\{\frac{\rho_1}{\nu}\right\}$ ratio was calculated. An arbitrarily chosen value of inner cylinder velocity therefore determined the kinematic viscosity required theoretically for instability.

The frictional-heating effect on the fluid was used to advantage. Setting the speed at a constant value which, for a known fluid viscosity, yielded an $\left\{\frac{\rho_1}{\nu}\right\}$ ratio slightly lower than that required for critical conditions, speed and torque values were recorded on the galvanometer. As the heating increased, the viscosity of the fluid gradually decreased, until instability, as detected by an increase in the recorded torque, was observed. The apparatus was then stopped and temperature measurements

were taken. From the recorded data at critical, the experimental $\left\{\frac{\rho_1}{v}\right\}$ ratio was established.

3.1 OBSERVATIONS AND RESULTS

The results obtained in both groups of experiments on steady-state motion were restricted by the present limitations of the apparatus and instrumentation. These included:

- (1) Noise associated with slip-ring and brush assembly.
- (2) The lack of a calibration for combined seal and bearing friction as a function of speed.
- (3) Unsuitability of present system of detecting torque where absolute values of the change in torque at transition are concerned.

3.11 Laminar Flow:

The experiments in this category were affected by the second limitation mentioned above. At low speeds and small heads of working fluid, the combined friction was negligible. At higher speed and under the full head, however, the seal and bearing contribution became significant. For a given head of fluid, it seemed reasonable to assume that this value would be a function of speed.

A calibration of this effect was required in order to obtain quantitative results. The method involved would be one which produced a given head on the seal over the expected speed range without introducing a fluid torque of any consequence. One suitable alternative appeared to be the use of compressed air as the working medium. Each alternative, however, required considerable modification to the existing apparatus.

As a result, the experiments were carried out without the necessary calibration and consequently, absolute values were not obtained. However, it was possible through the series of experiments to show that, once the mechanical friction was accounted for, dependable results seemed certain. Table I shows a typical set of results based on experiments run at roughly a constant speed under a 61 cm. head of a 55% "Pluracol"-water solution.

TABLE I

TEST	Speed (RPM)	μ (Centipoise)	h (Cm.)	G _{expt.} (Kg.Cm.)	G _(theor.) (Kg.Cm.)	ΔG (Kg.Cm.)
1	441	1853	61	8.72	5.61	3.11
2	444	1875	61	8.86	5.72	3.14
3	445	1890	61	8.90	5.78	3.12
4	444	1890	61	8.88	5.76	3.12

Capillary-tube viscometers and a constant-temperature bath were used to obtain the fluid viscosity. These measurements were taken immediately following a set of experiments.)

The value of $G_{\text{expt.}}$ was that recorded on the galvanometer trace - the absolute value being read from the torque versus deflection calibration curve. $G_{\text{theor.}}$ was the value obtained by inserting the appropriate experimental values into expression (1). (Section 3, page 10). The values of ΔG , which represent the combination bearing and seal frictions at the given speed are constant to $\pm 1\%$ and, as expected, decreased in magnitude at lower speeds (eg. 1.99 kg.cm. at 345 RPM).

From these results it would appear as if the reliability of the instrumentation is quite reasonable. Although the values listed in Table I effectively give only an indication of the repeatability of the combined system, the majority of the total error was expected to appear in the form of random error - most of which has been accounted for in these experiments.

Systematic errors, if any, will arise with quantitative results, and in general they are eliminated relatively easily.

3.12 Stability Experiments:

Owing to the amount of noise associated with the slip-ring and brush assembly, the experiments in which the stability of flow was examined were limited to those in which the inner cylinder was rotated at constant speed while the outer cylinder remained stationary. The solution to this problem lies in either isolating the slip-ring assembly from the main body of the apparatus or in purchasing a more robust unit.

With cylinder radii of 2.722 cm. and 1.992 cm., the critical $\left(\frac{\Omega_1}{V}\right)$ ratio of the apparatus is given by theory derived for 'wide-gap' configurations, and involves a trial and error solution of the set of equations mentioned previously. (See Chandrasekhar's 'Hydrodynamic and Hydromagnetic Stability', Pg. 320.) However, while a similar set of equations can result when dealing with 'narrow-gap' geometries, there are also expressions predicting the onset of instability in this category which lend themselves more favourably to an analytical solution - these expressions also giving a good approximation to the critical ratio for the wide-gap cases. In the present experiments, an extrapolation of expressions derived by G.I. Taylor⁽³⁾ and L. Prandtl⁽⁴⁾

gave the approximate ratio of $\left\{\frac{l_1}{V}\right\}$ to be 52 for $u = \left\{\frac{l_2}{l_1}\right\} = 0$.

The experimental procedure was as outlined previously in this section. It was found, however, that the instrumentation selected for recording the small change in torque as the fluid breakdown occurred was not developed sufficiently to obtain meaningful quantitative results. With the existing system it was possible to detect the change; however, in all cases this was not only a small percentage of the torque level, but was also a relatively small quantity when compared with the system noise, (largely owing to the slip-ring assembly). As a result, torque levels of approximately 2 cm. on the galvanometer were increasing by only 0.04 cm., while the peak to peak noise amounted to 0.4 cm. With the strain-gauge calibration accurate to $\pm 1\%$, the absolute value of this torque increment was not significant.

A suitable modification to the existing system, which would undoubtedly prove successful, uses a similar electric circuit to that designed as part of the clutch control unit. In applying this circuit, the torque associated with laminar flow conditions immediately preceeding the transition, and expressed as a voltage from

the strain-gauge-amplifier circuit, could be recorded - and then backed off. An amplifying stage would then be inserted into the system resulting in amplification of the small change in torque as the breakdown occurred. The output of the circuit could then be recorded on an oscilloscope, or once again be used to drive the recording galvanometer. :

Although the transition could not be detected effectively using the existing instrumentation, it was interesting to note that by using water-glycerin solutions with a relatively high degree of entrained air, the formation of vortices could be observed visually with no difficulty. The observations were exactly those which Taylor recorded originally. The initial disturbance resulted in equally-spaced "bands" of width approximately equal to the wavelength of the disturbance in the axial direction. (see Fig. 6). As the viscosity of the liquid continued to decrease, each band was divided equally, and the cellular vortex pattern was established. The resulting configuration is shown in Fig. 7.

It was interesting to note, that, when in the initial stages of development (i.e. divided into wide bands), the disturbance did not appear to affect the

usual concentric-circle-streamline pattern of cylindrical laminar flow. Only when the wide bands divided into the individual cells were the streamlines altered into individual vortices; however, even then, the flow appeared laminar. From the observations based on these experiments, therefore, the formation of vortices is accompanied by a change in the flow pattern while the state of the motion remains unaltered. Only at much higher cylinder speeds does turbulent flow prevail.

Table II gives representative experimentally-determined critical ratios - the solutions used in these cases being 84 - 86% glycerin by weight. The defined "critical" was taken in these experiments to be the point at which the individual vortices first appeared.

TABLE II

Test	Speed (Revs/Min)	$v \times 10^2$ (cm. ² /sec)	$\left\{ \frac{\rho l}{v} \right\}$ crit.
1	365	73.1	52.3
2	379	74.9	53.0
3	380	75.6	52.7
4	385	74.5	54.0
5	390	77.5	52.7
6	484	95.9	52.9

A mean value taken over the total number of experiments produced a ratio of 52.9 - the ratios contributing to this figure all falling within a range of $\pm 2\%$.

It may also be noted that, through the narrow-gap expressions, the onset of instability was predicted within 2% of the experimentally-observed value.

3.2 SUMMARY OF STEADY-STATE EXPERIMENTS

With a correction to the present limiting factors in the apparatus and instrumentation, and additions where existing instrumentation has proved inadequate, the entire system constructed would appear to be capable of producing reliable quantitative results. This should apply for experiments conducted previously in this category, as well as for those in which apparatus limitations, to date, have prevented an investigation. Possibly the best example of this is the usefulness of this system in detecting and recording torques in steady-state cylindrical motion where both cylinders are rotated simultaneously. The use of torsion balances and dead-weights used previously as a means of obtaining torque values are unsuitable for experiments of this nature.

4. ACCELERATED FLOW

The study of the mechanics of motion of either solid or fluid bodies in most cases is simplified considerably when the action takes place under a constant force or where uniform motion is involved. With this in mind therefore, it appeared reasonable to approach investigations into accelerated cylindrical flows by considering the cylinder motion either under the action of a constant couple, or when moving with constant angular acceleration. It was for this reason that an induction clutch capable of producing both constant torque and acceleration was selected.

4.1 PROPOSED EXPERIMENTS

A theoretical analysis by Professor T.H. Havelock forms the basis for the preliminary series of experiments in this category. In Havelock's paper, outlined in Appendix I, the author has considered the motion of a hollow cylinder containing a viscous fluid, when accelerated from rest under the action of a constant torque.

Once the constant-torque control circuit for the induction clutch has been completed, the apparatus

will be capable of simulating experimentally the conditions outlined in the theoretical treatment. An analysis of the problem from an experimental viewpoint was therefore undertaken.

Considering the cylinder acceleration as a function of the remaining system parameters, the problem could be expressed as follows:

$$\alpha = f(N, I, a, u, \rho, t)$$

where:

N represented the constant driving torque/unit cylinder length.

I represented the cylinder inertia/unit cylinder length.

a represented the cylinder radius.

u represented the dynamic viscosity of the fluid.

ρ represented the fluid density.

t represented the time.

Dimensional analysis on the above expression showed that four non-dimensional groups were sufficient to define the problem. These included:

$$\left\{ \frac{I\alpha}{N} \right\} ; \left\{ \frac{ua^2}{NI} \right\} ; \left\{ \frac{\rho a^4}{I} \right\} ; \left\{ \sqrt{\frac{N}{I}} t \right\}$$

Referring to equation 16 in Appendix 1, it may be seen that the exact analysis enabled the cylinder acceleration to be expressed as a function of a particular

combination of these groups; namely:

$$\alpha = \frac{N}{I} \psi \left\{ \frac{ua^2}{\sqrt{NI}} \cdot \sqrt{\frac{N}{I}} t ; \frac{\rho a^4}{I} \right\}$$

which, for a constant value of $\frac{\rho a^4}{I}$ reduced to the form:

$$\alpha = \frac{N}{I} \phi \left\{ \frac{vt}{a^2} \right\} \quad (2)$$

where $v = \frac{\mu}{\rho}$; the kinematic viscosity of the fluid.

Through equation (2), a graphical representation of both theoretical values and experimental results

could be obtained by plotting $\left\{ \frac{I\alpha}{N} \right\}$ against $\left\{ \frac{vt}{a^2} \right\}$

for various values of $\frac{\rho a^4}{I}$ (or preferably against

'K' = $\frac{2\pi\rho a^4}{I}$ - the exact value of this parameter.)

With the lack of uniformity in the outer-cylinder assembly, the cylinder inertia to be used in a comparison would best be determined experimentally. By accelerating the cylinder under a constant torque, the corresponding acceleration could be determined from the galvanometer trace.

Although the inertia could be changed by either adding to or subtracting from the present arrangement, essentially both the cylinder inertia and its radius

would be constants. The primary variables which could be controlled would be the torque and fluid density, and for experimental purposes suitable ranges of these could be chosen to provide a reasonable range of 'K' and ' α '.

An approximation to the actual cylinder inertia was made by calculation, and with the measured cylinder radius, and with an arbitrarily chosen value of torque, a hypothetical set of curves for solutions over the water-glycerin range at 25°C was produced.

In order to determine the parameters based on Havelock's theoretical analysis, a solution of equation (16) of Appendix I was required. This involved finding a sufficient number of values of λ , for any 'K' and given set of remaining variables, to obtain convergence of the infinite series.

A summation over the first twenty roots of equation (8) was found to be sufficient for the range of 'K' and conditions expected, not only in this one case, but in the probable experiments to be run on the apparatus in the future. From approximations, the exact values of the roots were determined by Newton's method.

This operation, and the subsequent solution of equation (16) involved a considerable amount of work for each value of acceleration produced. A programme was therefore written for the 'Deuce' computer, from which the roots, and the solution to the equation for a series of values of 't' could be obtained. A flow diagram of the programme is shown in Appendix III. The computed results based on the hypothetical group of variables for water, 50%, 75% and 100% water-glycerin solutions are given in Figure 8.

4.2 GENERAL DISCUSSION

Referring to Havelock's equation (16), the cylinder acceleration at any time 't' is expressed as the sum of two terms; one independent of time, the other a function of time. For sufficiently large values of $\frac{vt}{a}$, the cylinder acceleration reduces to a constant value corresponding to a rigid-body acceleration of the combined fluid and cylinder inertias. The form of the equation also suggests that the shearing stresses within the fluid gradually increase with time through the "transient" period, for by differentiating equation (17) of the appendix partially with respect to r and in

particular, setting $r = a$, it is seen the negative sign preceding the second term will remain for all values of 't' provided:

$$\left\{ \frac{\lambda J_1'(\lambda)}{J_1(\lambda)} - 1 \right\} > 0.$$

Since by equation (8) in the Appendix, the positive roots of the equation are restricted to values of λ where $J_1(\lambda)$ and $J_2(\lambda)$ are of opposite sign, the above expression is always positive.

Once at the large values of $\frac{vt}{a^2}$, the shear distribution is fixed. By considering the net torque acting on any element within the body of fluid, and summing this over the total fluid enclosed by the cylinder, it is found that the time rate of change of angular momentum of the fluid is a constant - the portion of the applied torque allotted to fluid acceleration being directly proportional to the total fluid inertia. This result immediately suggests that the shear-stress distribution is a function of the fluid density and must be independent of its viscosity. This should apply for all Newtonian fluids. However, no conclusion can be drawn from the above on the probable behavior of non-Newtonian or thixotropic fluids under the same type of

motion, as the mathematical analysis was based on the assumption of a viscosity independent of rates of strain within the fluid.

The degree of correlation between the theoretical and experimental results will not only depend on the apparatus simulating the experimental conditions, but will also depend on the fluid behaving in the manner assumed in the derivation. McLeod⁽⁶⁾ in his investigation into cylindrical motion, observed that on starting a cylinder containing water from rest, and on stopping it suddenly when rotating at a constant speed, a considerable amount of turbulence resulted. In this case, the turbulence would transfer additional momentum, resulting in a more rapid overall transfer of momentum than that taking place under the sole influence of laminar shear. It might therefore be expected that the experimentally-determined curve would be of greater slope in the "transient" section with the terminal acceleration being reached in advance of that predicted by the laminar theory.

It is of interest to compare the energy dissipation in the combined fluid-solid system rotating at a constant acceleration with that of a solid body under the same

acceleration. Whereas a solid body being accelerated under a constant torque dissipates energy at a rate proportional to the increase in strain and kinetic energies of the system, the combined system involves an increase in kinetic and pressure energies, as well as a dissipation owing to the viscous effects within the fluid. In the case of a solid body, the increase in strain energy is generally small relative to the gain in kinetic energy, and therefore the total dissipation can be assumed to appear as an increase in kinetic energy -- the rigid-body case.

The increase of pressure energy in the combined system is associated with a change in shape of the free surface, and therefore when energy input into a sufficiently long cylinder is being considered, only kinetic energy and viscous dissipation are significant. With the viscous term expressed as:

$$\int_0^a 2\pi\mu r^3 \left\{ \frac{\partial v}{\partial r} \right\}^2 dr,$$

the dissipation, once fixed shear-stress distribution has been established, is constant, and since the rate of power dissipation for the two systems is identical, the increase in kinetic energy of the combined system differs

from that of the equivalent solid body by this viscous effect.

4.3 FUTURE PROGRAMME

In another particular case of accelerated motion, a hollow cylinder containing a viscous liquid being accelerated at a constant rate, may be examined using equation (1) of Appendix I. The equation of motion

$$\Omega'(t) + \frac{4\pi\mu a^2}{I} \int_0^t \Omega'(\tau) \sum e^{-\frac{v p^2 (t-\tau)}{a^2}} d\tau = \frac{N}{I} \quad (3)$$

(where N is now a variable), may be solved without the use of a solving function since $\Omega'(t) = \Omega'(\tau)$, the constant cylinder acceleration. Carrying out the integration in equation (3) leads to:

$$N = I \Omega'(t) \left\{ 1 + \frac{4\pi\mu a^2}{I} \sum \frac{a^2}{v p^2} \left(1 - e^{-\frac{v p^2 t}{a^2}} \right) \right\} \quad (4)$$

where, as in equation (3), the summation extends over the positive roots of $\frac{1}{p} J_1(p) = 0$. Noting that the summation of $\frac{1}{p^2}$ converges to $1/8$, it is seen that, for sufficiently large values of $\frac{vt}{a^2}$, the total driving torque increases to a constant corresponding to that required to accelerate

an equivalent rigid body. As in the case of acceleration under constant torque, the shear-stress distribution becomes independent of viscosity, and the time rate of change of angular momentum for the entire fluid is a constant.

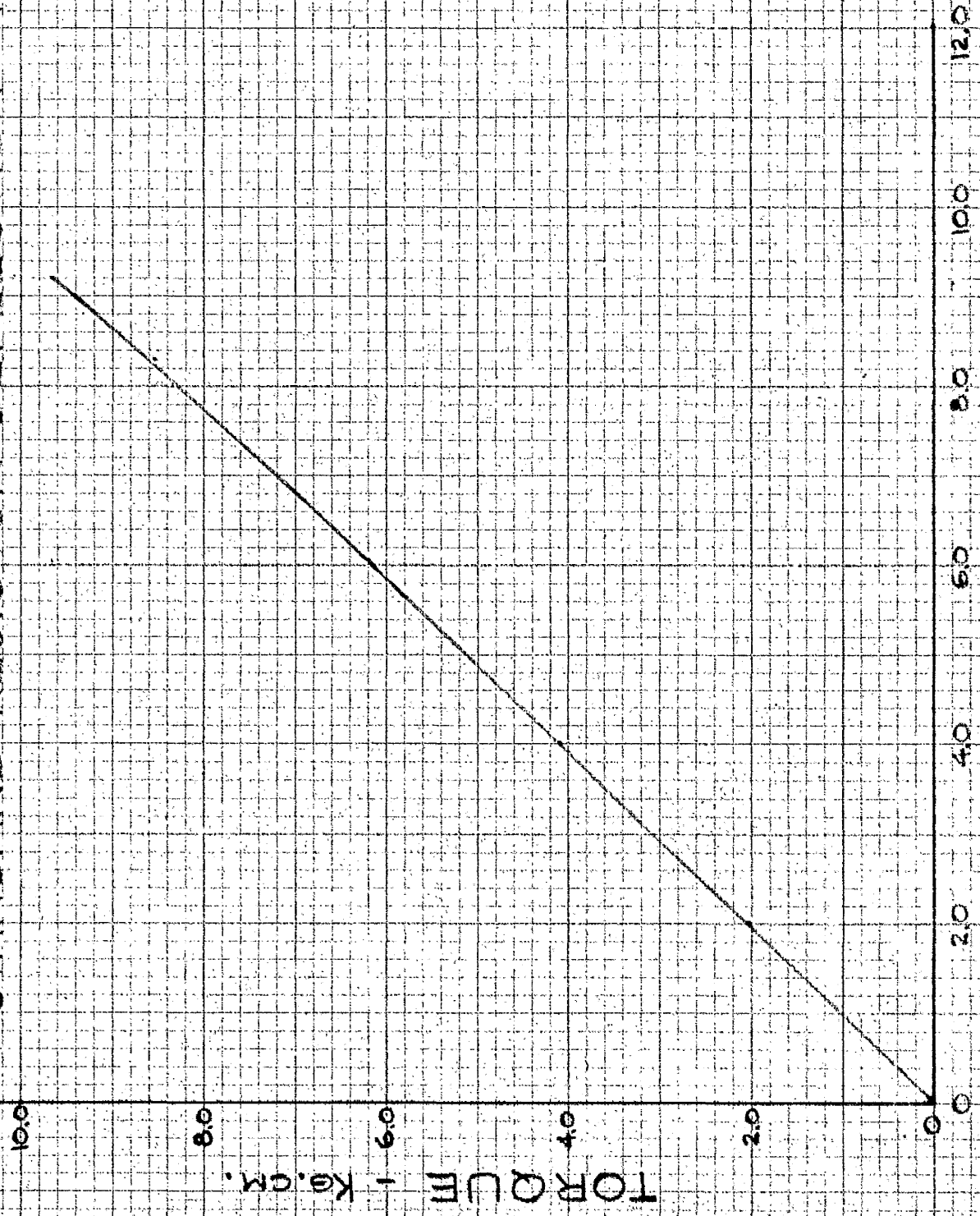
It would appear that the most logical approach to the complete study of flows in this category would be to examine theoretically the general case of flows acting under the influence of boundaries either being driven by a constant torque or moving with constant acceleration. This would give complete coverage of the laminar flows, thus providing the necessary base for considering instability in this type of motion.

Nothing can be predicted regarding the stability of accelerated motion at present. However, in the limited cases considered, the existence of a well-defined distribution of angular momentum once the transient stage has been overcome, is encouraging. Based on the importance of the distribution of angular momentum in the case of unstable motion under steady-state conditions, the distribution undoubtedly will represent an important factor in the study of the stability of accelerated flow.

STRAIN-GAUGE CALIBRATION

CARRIER-AMPLIFIER CHANNEL 2

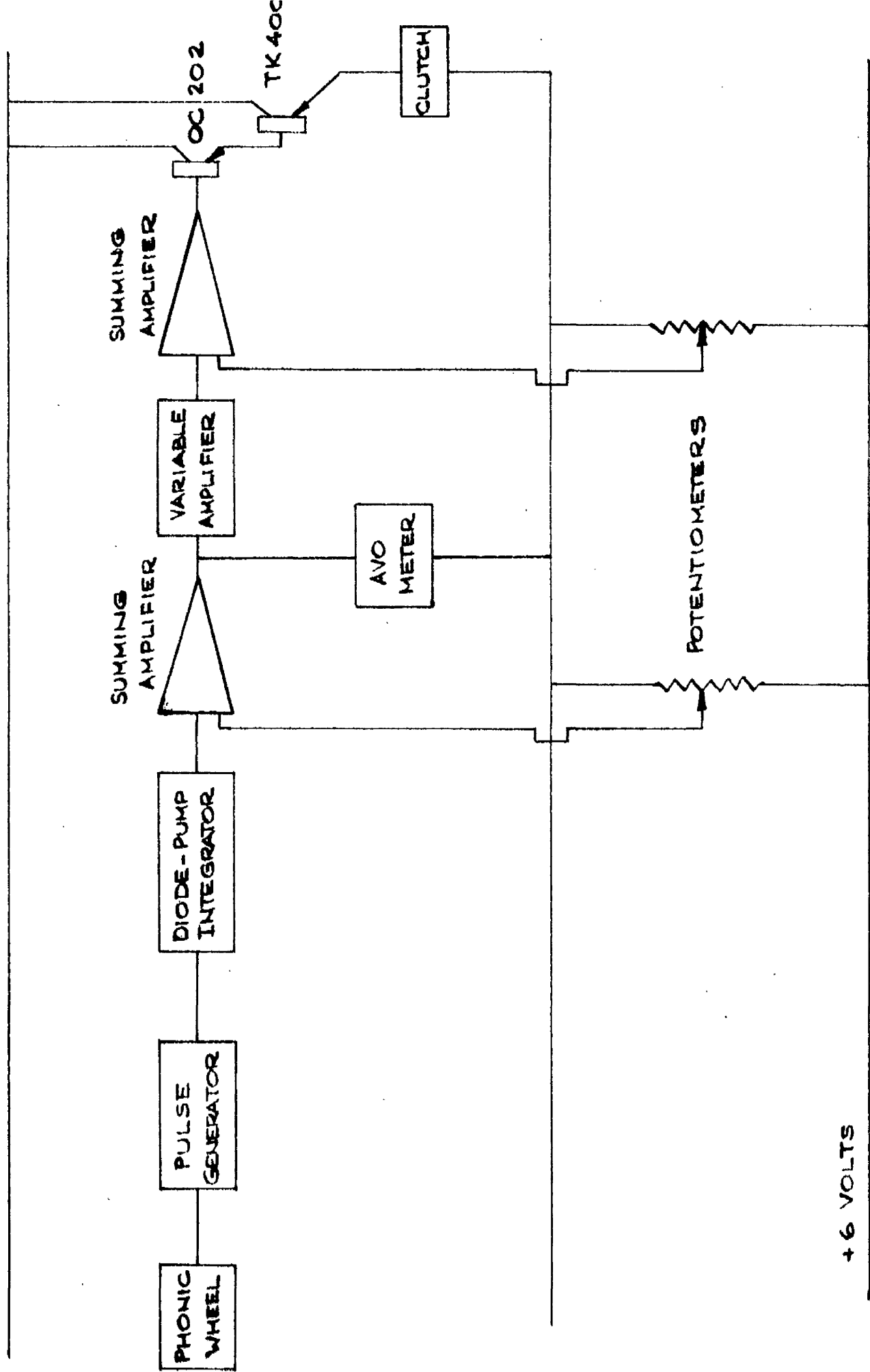
STANDARD RESISTOR DEFLECTION = 7.33 CM.



GALVO. DEFLECTION - CM.

FIG. 1

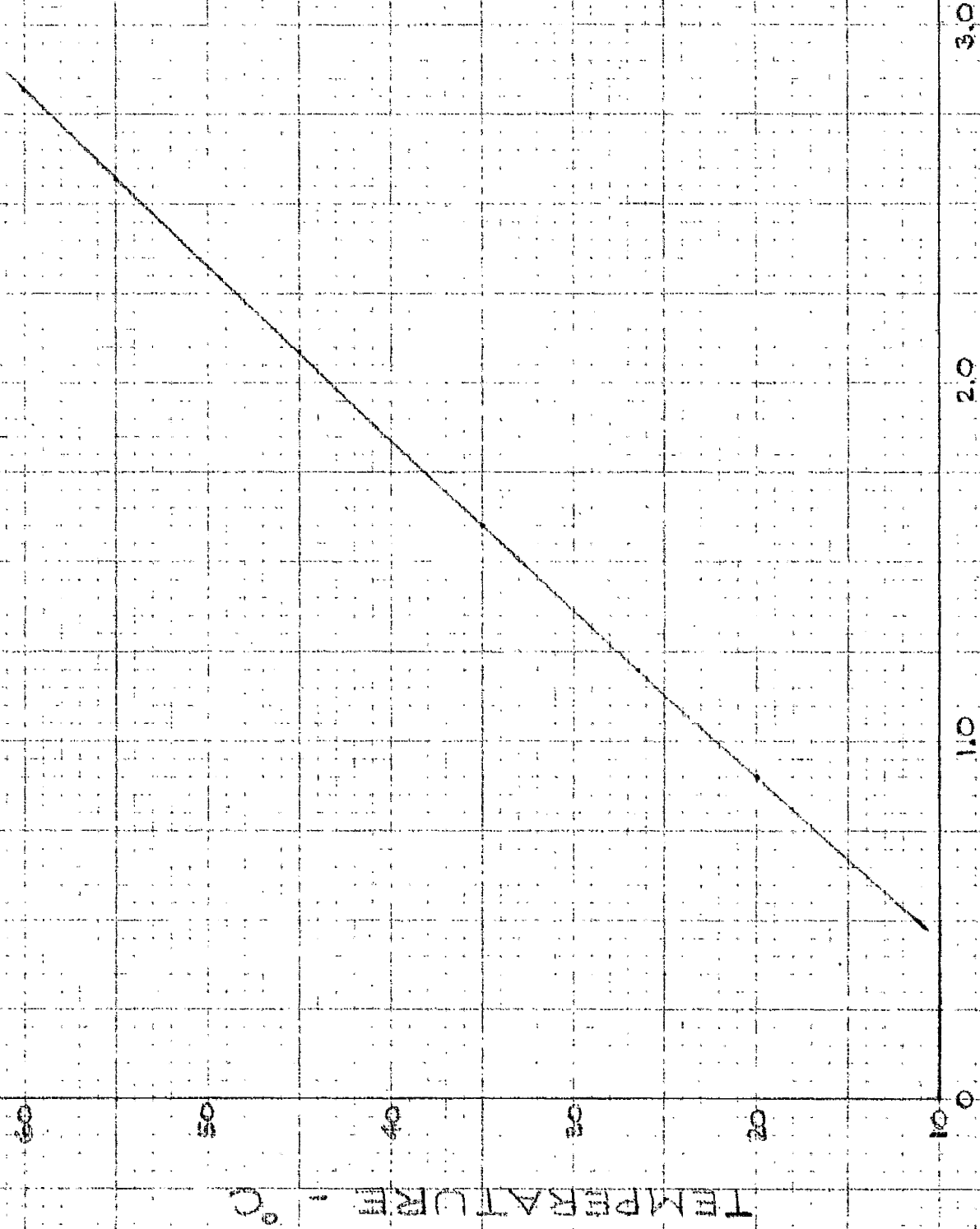
-12 VOLTS



SPEED CONTROL CIRCUIT

FIG. 2

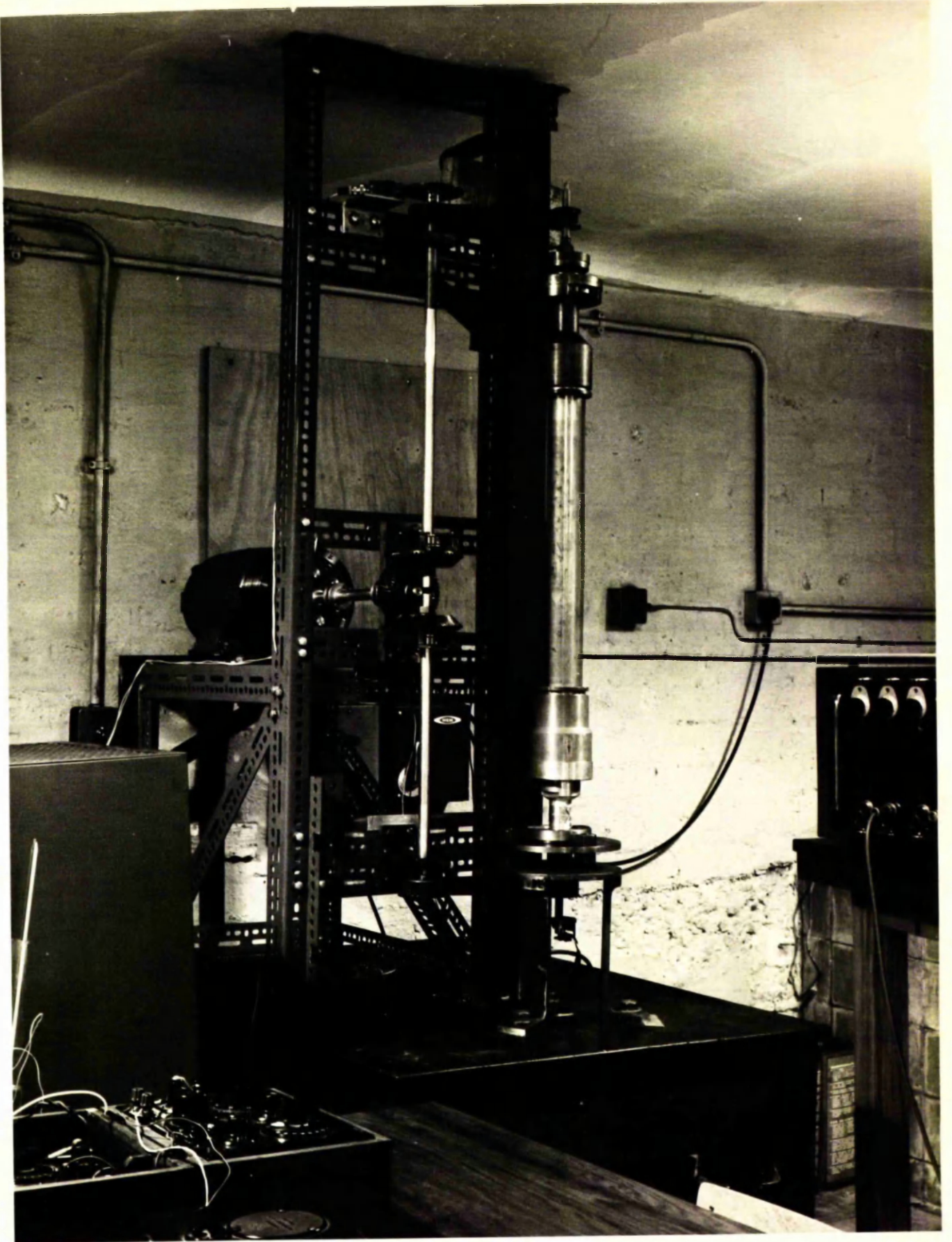
THERMOCOUPLE CALIBRATION



OUTPUT - MV.

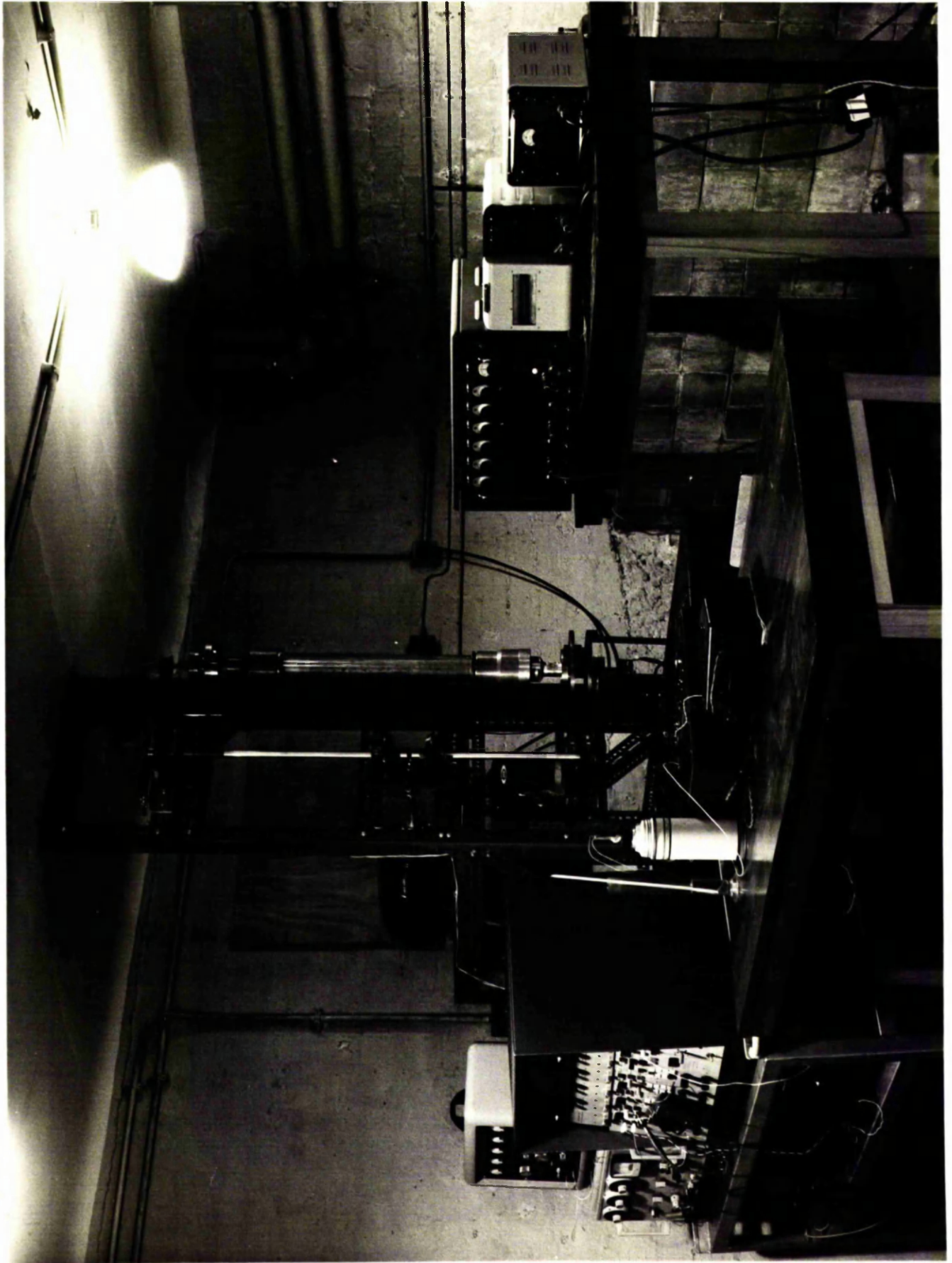
FIG 3

FIG. 4



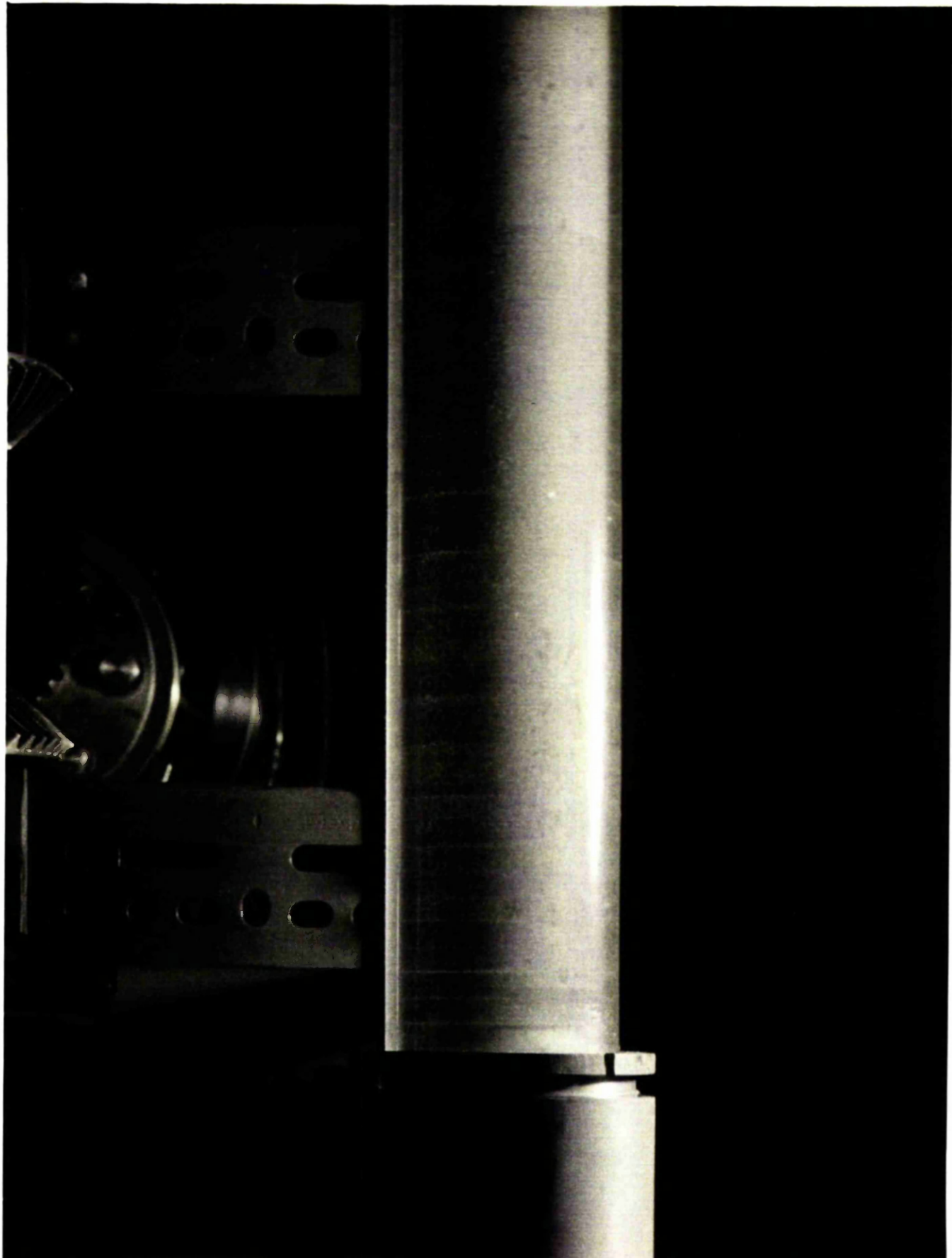
CYLINDER ASSEMBLY AND ASSOCIATED DRIVE

FIG. 5



GENERAL LAYOUT OF APPARATUS AND AUXILIARY EQUIPMENT

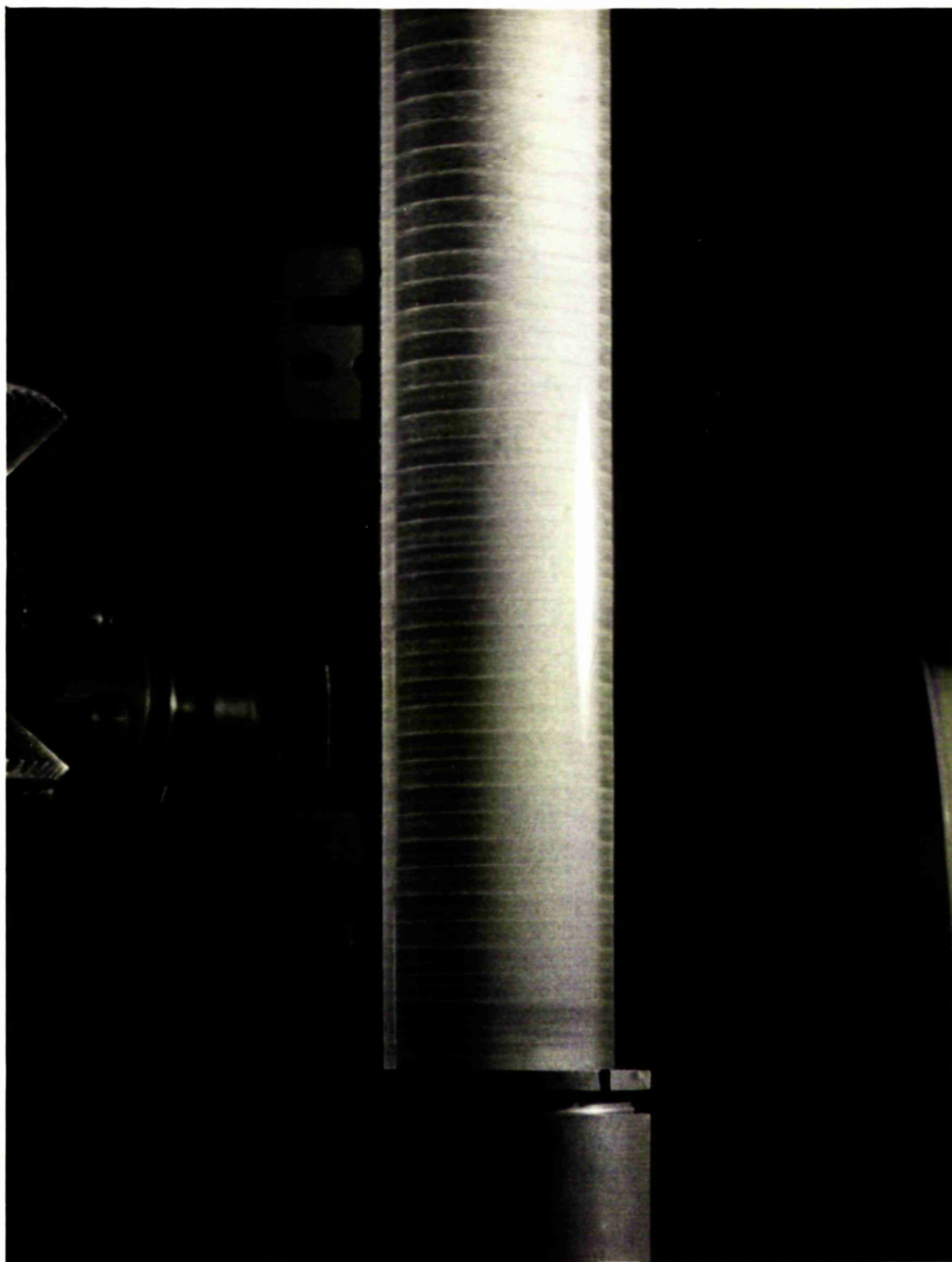
FIG. 6



INITIAL STAGE OF FLUID INSTABILITY

$u = 0$; $N_1 = 400$ RPM

FIG. 7



FULLY-DEVELOPED VORTEX PATTERN INDICATING COMPLETE INSTABILITY

$u = 0$; $N_1 = 400$ RPM

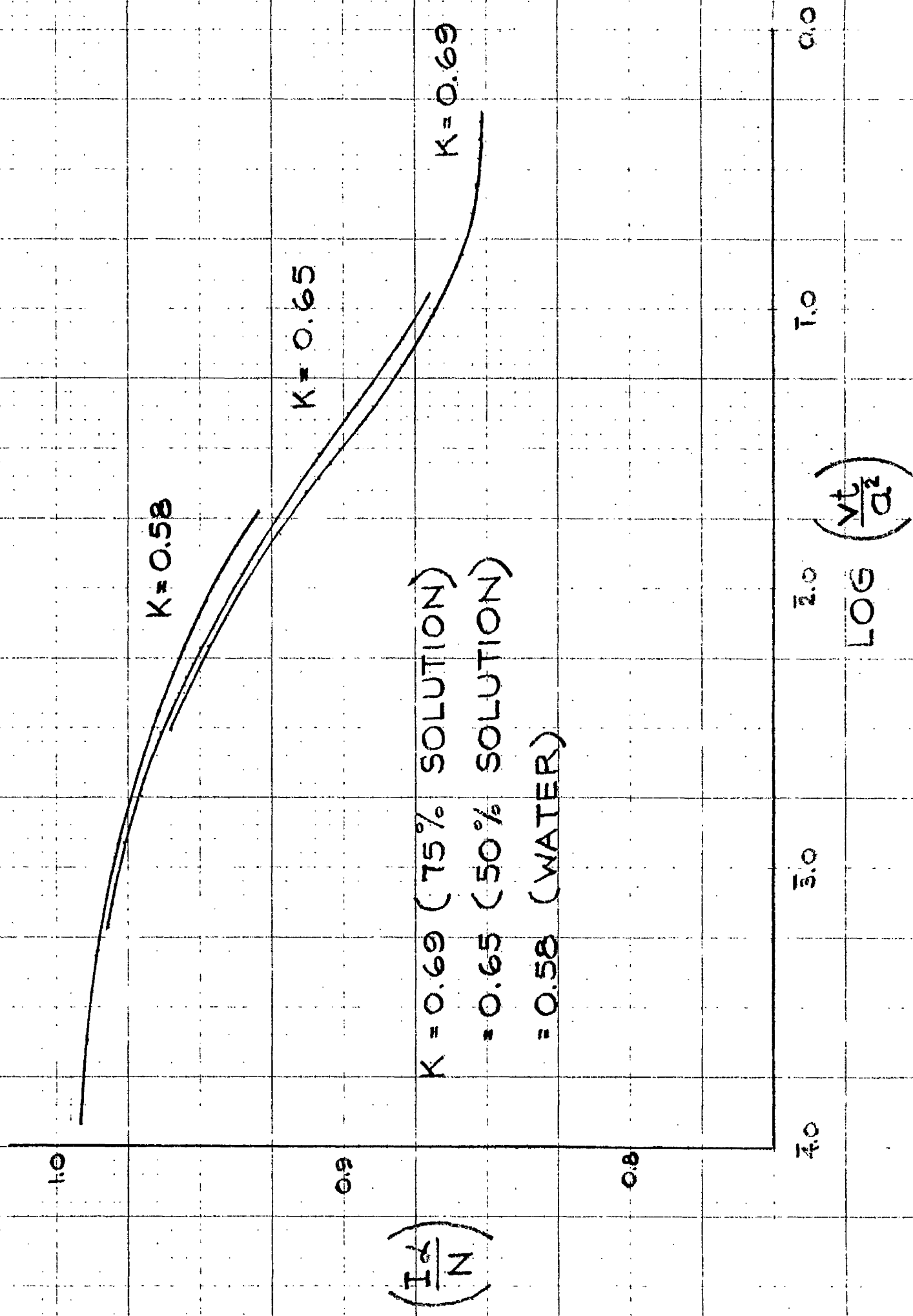


FIG. 8. THEORETICAL ACCELERATED MOTION

APPENDIX I

In the paper by Professor T.H. Havelock, axisymmetric cylindrical motion of a fluid satisfying the following expression is considered:

$$\frac{\partial v}{\partial t} = v \left\{ \frac{\partial^2 v}{\partial r^2} + \frac{1}{r} \frac{\partial v}{\partial r} - \frac{v}{r^2} \right\}$$

The symbol 'v' represents the fluid velocity, perpendicular to the radius vector, "r".

With motion starting from rest, it is shown that, at any time "t", the angular velocity of a fluid contained in a hollow cylinder of radius "a", and having angular velocity $\Omega(t)$, is given by:

$$w = \int_0^t \Omega(\tau) \left\{ 1 + 2 \sum_{pr} \frac{a J_1(pr/a)}{J_1(p)} e^{-\frac{v p^2 (t-\tau)}{a^2}} \right\} a \tau \quad (1)$$

where the summation extends over the positive roots of $J_1(p) = 0$.

Acceleration of the cylinder, under the action of a constant couple W, is then considered. Analysis of the forces on the cylinder, assuming a fluid friction retarding couple of the form $2\pi r^3 \frac{\partial w}{\partial r}$ leads to an equation of motion for the cylinder:

$$l'(t) + \frac{4\pi u a^2}{I} \int_0^t l'(\tau) \sum e^{-\frac{vp^2}{a^2}(t-\tau)} d\tau = \frac{N}{I} \quad (2)$$

where both N and I are values/unit cylinder length, and where the summation extends over the positive roots of $\frac{1}{p} J_1(p) = 0$.

It should be noted that the summation excludes the root $p = 0$. Although, in effect, the summation should still be over the zeros of $J_1(p)$ including the value zero, it can be shown that this particular root has no bearing on the value of the integral.

Considering the term concerning the value $p \rightarrow 0$ in expression (1). Neglecting the summation sign, a consideration of the single term:

$$\Phi(w) = \int_0^t l'(\tau) \left\{ 1 + 2 \left\{ \lim_{p \rightarrow 0} \frac{a J_1(pr/a)}{pr J_1(p)} \right\} e^{-\frac{vp^2}{a^2}(t-\tau)} \right\} d\tau$$

represents the contribution of the zero root to the value of w .

In differentiating both numerator and denominator of the expression in square parenthesis, the $\lim_{p \rightarrow 0}$ is seen to equal 1. It may then be seen that by differentiating

partially with respect to "x" ; $-\Phi'(w) = 0$; and therefore can be neglected in equation (2).

This result enables equation (2), an integral equation of Poisson's type, to be solved accordingly, in a manner suggested by E.T. Whittaker⁽⁷⁾. Whittaker considers an equation:

$$\Phi(x) + \int_0^x \Phi(s) k(x-s) ds = f(x) \quad (3)$$

in which the nucleus is a sum of n exponentials:

$$\text{i.e. } k(x) = P e^{px} + Q e^{qx} + \dots + \dots + V e^{vx}$$

The solution can be written:

$$\Phi(x) = f(x) - \int_0^x f(s) K(x-s) ds \quad (4)$$

where $K(x)$ is also a sum of v exponentials, or:

$$K(x) = A e^{\alpha x} + B e^{\beta x} + \dots + \dots + N e^{v x}$$

Whittaker then shows that the exponents $\alpha, \beta, \gamma, \dots, v$, of the solving function are the roots of the equation:

$$\frac{P}{x-p} + \frac{Q}{x-q} + \dots + \dots + \frac{V}{x-n} + 1 = 0 \quad (5)$$

while the coefficients in $K(x)$ satisfy the equations:

$$\frac{A}{\alpha-p} + \frac{B}{\beta-p} + \dots + \dots + \frac{N}{v-p} + 1 = 0$$

$$\frac{A}{\alpha-n} + \frac{B}{\beta-n} + \dots + \dots + \frac{N}{v-n} + 1 = 0 \quad (6)$$

From equation (2), the appropriate form of equation (5) is seen to be:

$$\frac{4\pi\nu a^4}{I} \left\{ \frac{1}{a^2\kappa + \nu p_1^2} + \frac{1}{a^2\kappa + \nu p_1^2} + \dots \right\} + 1 = 0 \quad (7)$$

Substituting, $\kappa = \frac{\nu\lambda^2}{a^2}$, Havelock reduces the

resultant equation into:

$$KJ_2(\lambda) + \lambda J_1(\lambda) = 0 \quad (8)$$

where $K = 2\pi\nu a^4/I$. This conclusion can be verified as follows from (8):

$$1 + \frac{KJ_2(\lambda)}{\lambda J_1(\lambda)} = 0$$

Substituting $J_2(\lambda) = \frac{1}{\lambda} J_1(\lambda) - J_1'(\lambda)$ leads to:

$$\begin{aligned} 0 &= 1 - \frac{K}{J_1(\lambda)} \left\{ -\frac{1}{\lambda^2} J_1(\lambda) + \frac{J_1'(\lambda)}{\lambda} \right\} \\ &= 1 - \frac{K}{J_1(\lambda)} \frac{\partial}{\partial \lambda} \left\{ \frac{J_1(\lambda)}{\lambda} \right\} \\ &= 1 - \frac{K\lambda}{\lambda J_1(\lambda)} \frac{\partial}{\partial \lambda} \left\{ \frac{J_1(\lambda)}{\lambda} \right\} \\ &= 1 - \frac{K}{\lambda} \frac{d}{d\lambda} \ln \left\{ \frac{J_1(\lambda)}{\lambda} \right\} \end{aligned} \quad (9)$$

Remembering that in equation (2), the summation extended over the positive roots of $\frac{1}{p} J_1(p) = 0$,

equation (9) can therefore be written:

$$\begin{aligned}
 0 &= 1 - \frac{K}{\lambda} \frac{d}{d\lambda} \ln \left\{ G_n (\lambda - p_n)(\lambda + p_n) \right\} \\
 &= 1 - \sum_n \frac{K}{\lambda} \left\{ \frac{1}{\lambda^2 - p_n^2} \cdot 2\lambda \right\} \\
 &= 1 + \sum_n 2K \left\{ \frac{1}{-\lambda^2 + p_n^2} \right\}
 \end{aligned}$$

which is identical to the revised form of equation (7).

The coefficients of the solving function can be obtained from a set of equations of type (6), thus:

$$\begin{aligned}
 \frac{A_1}{\lambda_1^2 - p_1^2} + \frac{A_2}{\lambda_2^2 - p_2^2} + \dots + \dots - \frac{V}{a^2} &= 0 \\
 \frac{A_1}{\lambda_1^2 - p_v^2} + \frac{A_2}{\lambda_2^2 - p_v^2} + \dots - \frac{V}{a^2} &= 0 \quad (10)
 \end{aligned}$$

where the summations extend over the positive roots of

$\frac{1}{p} J_1(p) = 0$ and the positive roots of equation (8).

It may be noted that equation (8) may be written in the form:

$$(K + 2) J_2(\lambda) + \lambda J_2'(\lambda) = 0 \quad (11)$$

which can be identified as an equation yielding roots upon which a Dini expansion may be based.

Havelock, in his paper, uses the Dini expansion to solve equation (10), and assumes that a function $F(x)$ can be expanded, in the range $0 < x < 1$, in the series:

$$F(x) = \sum B J_2(\lambda x)$$

where the summation extends over the positive roots of (11).

From any reference on Dini expansions and using equation (11) it may be shown that the coefficients, B , will be given by the expression:

$$B = \frac{2\lambda^2}{\{\lambda^2 + K(K+4)\} J_2^2(\lambda)} \int_0^1 F(x) J_2(\lambda x) x dx \quad (12)$$

Havelock then takes $F(x) = J_2(px)$ where p is a positive root of $\frac{1}{p} J_1(p) = 0$. In the resulting expansion:

$$J_2(px) = \sum \frac{2\lambda^2}{\{\lambda^2 + K(K+4)\} J_2^2(\lambda)} \int_0^1 J_2(px) J_2(\lambda x) x dx$$

x is put equal to 1; also noting that:

$$\int_0^1 J_2(px) J_2(\lambda x) x dx = \frac{1}{(\lambda^2 - p^2)} \left\{ p J_2'(p) J_2(\lambda) - \lambda J_2'(\lambda) J_2(p) \right\}$$

the identity becomes:

$$J_2(p) = \sum \frac{2\lambda^2}{\{\lambda^2 + K(K+4)\} J_2^2(\lambda)} \left\{ \frac{1}{(\lambda^2 - p^2)} p J_2'(p) J_2(\lambda) - \lambda J_2'(\lambda) J_2(p) \right\}$$

with p being any root of $\frac{1}{p} J_1(p) = 0$ and the summation being with respect to the roots of equation (8), the above reduces to:

$$1 = \sum_{\lambda} \frac{2K\lambda^2}{(\lambda^2 + K(K+4))(\lambda^2 - p^2)} \quad (13)$$

Comparing equations (10) and (13), the coefficients of the solving function become:

$$A_B = \frac{2Kv\lambda^2}{B^2(\lambda^2 + K(K+4))}$$

Substitution in equation (2) yields:

$$\frac{d\lambda}{dt} = \frac{N}{I} - \frac{2KvN}{B^2 I} \int_0^t \sum \frac{\lambda^2 e^{-\frac{v\lambda^2}{a^2}(t-\tau)}}{\lambda^2 + K(K+4)} d\tau \quad (14)$$

where $\lambda^2(\tau) = \text{const.} = \frac{N}{I}$

By expanding r^2 by (12), and putting $r = 1$ the resulting identity is:

$$1 = \sum \frac{2(K+4)}{\lambda^2 + K(K+4)} \quad (15)$$

Integrating (14) and substituting from equation (15), it is found that:

$$\frac{d\lambda}{dt} = \frac{N}{1 + 1/2\pi pa^4} + \frac{2KN}{I} \sum \frac{e^{-\frac{v\lambda^2 t}{a^2}}}{\lambda^2 + K(K+4)} \quad (16)$$

The angular velocity of the liquid at any time is obtained by Havelock by integrating (16); giving the angular velocity of the cylinder, and then by using the initial differential equation:

$$\frac{\partial v}{\partial t} = v \left\{ \frac{\partial^2 v}{\partial r^2} + \frac{1}{r} \frac{\partial v}{\partial r} - \frac{v}{r^2} \right\}$$

with the result:

$$w = \frac{H}{I + 1/2\pi\rho a^4} \left\{ t + \frac{F^2}{8v} - \frac{K+6}{12(K+4)} \right. \\ \left. - \frac{v\lambda^2 t}{a^2} \right. \\ \left. - \frac{2KH}{I} \sum \frac{a^3 J_1(\lambda r/a) e^{-\lambda^2 t}}{v F^2 (\lambda^2 + K(K+4)) J_1(\lambda)} \right\} \quad (17)$$

APPENDIX II

An approximate method derived by Dunkerley, was used to determine the critical speeds of the assemblies. This method states that:

$$\frac{1}{n_c^2} = \frac{1}{n_1^2} + \frac{1}{n_2^2} + \frac{1}{n_3^2} + \dots$$

where n_c is the lower critical speed of the system.

n_1, n_2, n_3, \dots are the critical speeds on considering only one of the concentrated masses of the system.

In the case of both cylinders, two simplifying assumptions were made.

1. The assemblies were assumed to be simply-supported at their bearings.
2. Distributed loads were represented by a series of point loads. (7 in the case of the inner shaft; 5 for the outer assembly.)

The total strain energy in a simply-supported beam is given by the expression:

$$U = \int \frac{M^2 dx}{2EI}$$

which, as a means of simplifying calculations can be

expressed as a summation:

$$U = \sum \frac{1}{EI} (Mdx) \times \left(\frac{M}{2} \right)$$

where Mdx represents the area of the bending moment diagram, and $\left(\frac{M}{2} \right)$ the ordinate of the centroid of the

element dx .

The Theorem of Castigliano, in conjunction with the total energy equation, was used to obtain the necessary deflections and resulting shaft stiffnesses. The Theorem states that, in an elastic system, the partial derivative of the strain energy with respect to any force in the system is equal to the deflection at the point of application of that force.

The overall procedure for determining the critical speeds was as follows:

1. A unit load 'P' was assumed acting at the point of application of one of the concentrated shaft masses.
2. The resulting bending moment diagram was produced, and the total strain energy equated.
3. The energy expression was differentiated partially with respect to P, yielding:

$$\frac{\partial U}{\partial P} = \delta = \text{constant} \times P$$

where δ was the resulting deflection at the point of application, from this expression the shaft stiffness "k" = $\frac{P}{\delta}$ was determined.

4. The natural frequency of the system was obtained by substituting the actual load "n" into the standard expression:

$$n = \sqrt{\frac{gk}{m}}$$

5. The process was repeated for each mass in the system, resulting in a number of values of n^2 .
6. Substitution in Dunkerley's expression:

$$\frac{1}{n_c^2} = \frac{1}{n_1^2} + \frac{1}{n_2^2} + \frac{1}{n_3^2} + \dots$$

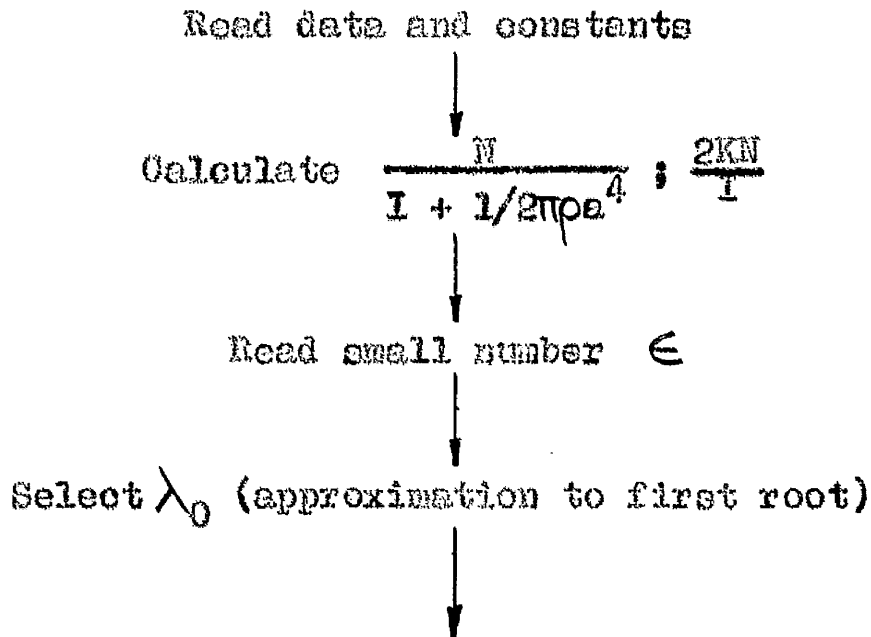
produced the lower critical speed of the system.

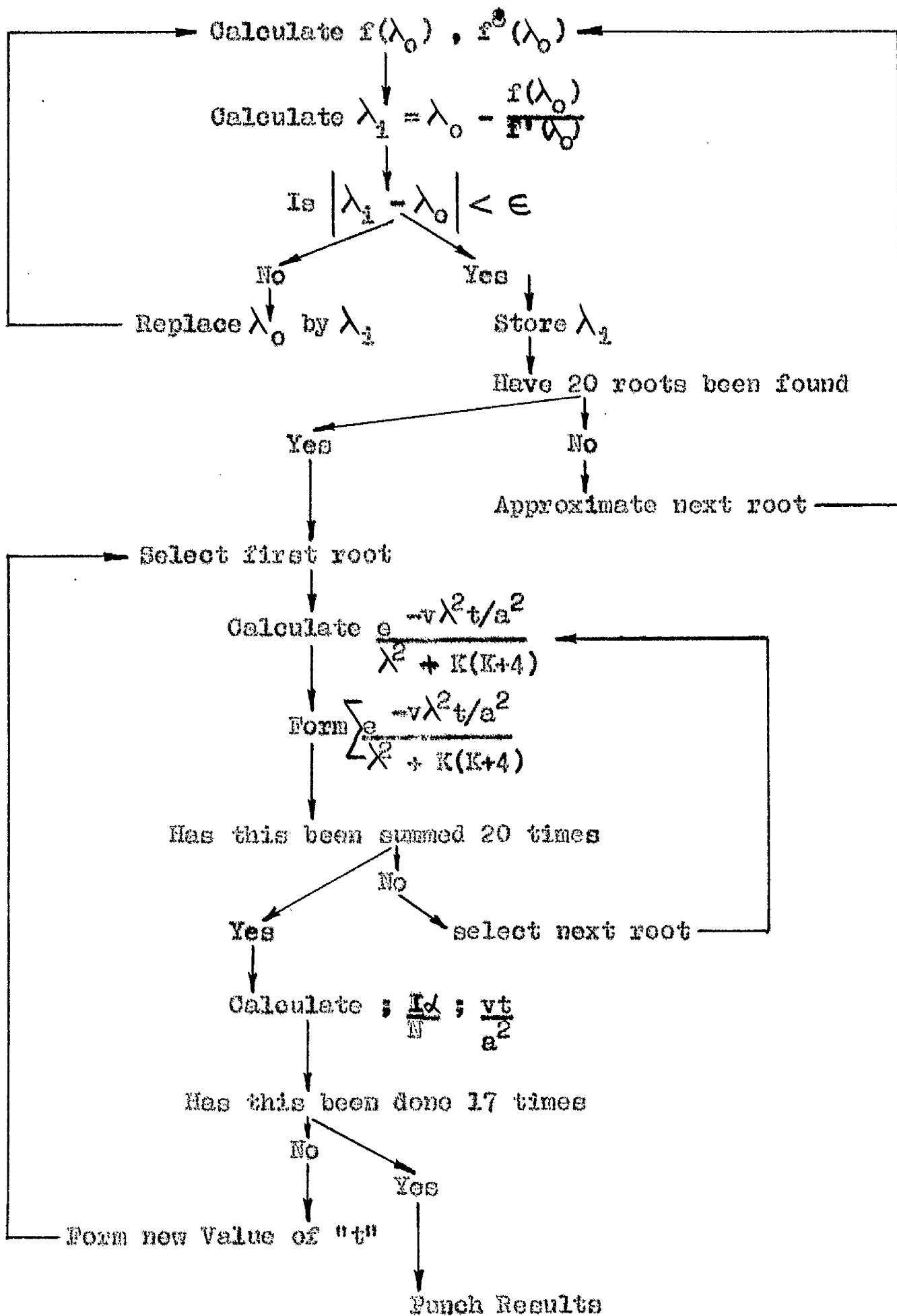
APPENDIX III

FLOW DIAGRAM FOR DIGITAL PROGRAMME.

$$\text{Solution of } \alpha = \frac{N}{I + 1/2\pi\rho e^4} + \frac{2KN}{I} \sum \frac{e^{-v\lambda^2 t/e^2}}{\lambda^2 + K(K+4)}$$

where the summation extends over the first twenty roots of: $KJ_2(\lambda) + \lambda J_1(\lambda) = 0 = f(\lambda)$, values of t from 0.1 (0.1) 1 (2) 15 seconds.





REFERENCES

1. Donnelly, R.J., Simon, M.J.; "An Empirical Torque Relation for Supercritical Flow Between Rotating Cylinders"; J. Fluid Mech. (7); pp. 40; (1960).
2. Chandrasekhar, S.; "Hydrodynamic and Hydromagnetic Stability"; Clarendon Press, 1961; pp. 272-342.
3. Taylor, G.I.; "Stability of a Viscous Liquid Contained Between Rotating Cylinders"; Trans. Roy. Soc.; London, a223; pp. 269-343; (1923).
4. Schlichting, H.; "Boundary Layer Theory"; McGraw-Hill; 1960; pp. 440.
5. Havelock, T.N.; "The Solution of an Integral Equation Occurring in Certain Problems of Viscous Fluid Motion"; Phil. Mag. 42; pp. 626-628 (1921).
6. McLeod, A.R.; "The Unsteady Motion Produced in a Uniformly Rotating Cylinder of Water by a Sudden Change in the Angular Velocity of the Boundary"; Phil. Mag. (6) 44; pp. 1-14; (1922).
7. Whittaker, E.T.; "On the Numerical Solution of Integral-Equations"; Proc. Roy. Soc. a; pp. 367, (1918).